

# Nonproteolytic Properties of Murine Alternatively Spliced Tissue Factor: Implications for Integrin-Mediated Signaling in Murine Models

Richard C Godby,<sup>1\*</sup> Yascha W van den Berg,<sup>2\*</sup> Ramprasad Srinivasan,<sup>1</sup> Robert Sturm,<sup>1</sup> David Y Hui,<sup>3</sup> Stephen F Konieczny,<sup>4</sup> Bruce J Aronow,<sup>5</sup> Evgeny Ozhegov,<sup>1</sup> Wolfram Ruf,<sup>6</sup> Henri H Versteeg,<sup>2\*</sup> and Vladimir Y Bogdanov<sup>1\*</sup>

<sup>1</sup>Department of Internal Medicine, Division of Hematology/Oncology, University of Cincinnati College of Medicine, Cincinnati, Ohio, United States of America; <sup>2</sup>Eindhoven Laboratory for Experimental Vascular Medicine, Leiden University Medical Center, Leiden, the Netherlands; <sup>3</sup>Department of Pathology and Laboratory Medicine, University of Cincinnati College of Medicine, Cincinnati, Ohio, United States of America; <sup>4</sup>Department of Biological Sciences and the Purdue Center for Cancer Research, Purdue University, West Lafayette, Indiana, United States of America; <sup>5</sup>Biomedical Informatics and Developmental Biology, Cincinnati Children's Hospital and Medical Center, Cincinnati, Ohio, United States of America; and <sup>6</sup>Department of Immunology, The Scripps Research Institute, La Jolla, California, United States of America

This study was performed to determine whether murine alternatively spliced tissue factor (masTF) acts analogously to human alternatively spliced tissue factor (hasTF) in promoting neovascularization via integrin ligation. Immunohistochemical evaluation of a spontaneous murine pancreatic ductal adenocarcinoma model revealed increased levels of masTF and murine full-length tissue factor (mflTF) in tumor lesions compared with benign pancreas; furthermore, masTF colocalized with mflTF in spontaneous aortic plaques of *Ldlr*<sup>-/-</sup> mice, indicating that masTF is likely involved in atherogenesis and tumorigenesis. Recombinant masTF was used to perform *in vitro* and *ex vivo* studies examining its integrin-mediated biologic activity. Murine endothelial cells (ECs) rapidly adhered to masTF in a  $\beta$ 3-dependent fashion. Using adult and embryonic murine ECs, masTF potentiated cell migration in transwell assays. Scratch assays were performed using murine and primary human ECs; the effects of masTF and hasTF were comparable in murine ECs, but in human ECs, the effects of hasTF were more pronounced. In aortic sprouting assays, the potency of masTF-triggered vessel growth was undistinguishable from that observed with hasTF. The proangiogenic effects of masTF were found to be Ccl2-mediated, yet independent of vascular endothelial growth factor. In murine ECs, masTF and hasTF upregulated genes involved in inflammatory responses; murine and human ECs stimulated with masTF and hasTF exhibited increased interaction with murine monocytic cells under orbital shear. We propose that masTF is a functional homolog of hasTF, exerting some of its key effects via  $\beta$ 3 integrins. Our findings have implications for the development of murine models to examine the interplay between blood coagulation, atherosclerosis and cancer.

Online address: <http://www.molmed.org>  
doi: 10.2119/molmed.2011.00416

## INTRODUCTION

Tissue factor (TF), an integral membrane glycoprotein, serves as an enzymatic cofactor of the serine protease

FVII/FVIIa and acts as the principle physiological trigger of the blood coagulation cascade. Aside from its role in the

maintenance of normal hemostasis and its involvement in a variety of thrombotic disorders, TF is known to affect angiogenesis via protease activated receptor-2 signaling and interactions with  $\alpha_3\beta_1$  and  $\alpha_6\beta_1$  integrins (1).

The term "angiogenesis" collectively refers to the processes that result in the formation of new vasculature from pre-existing blood vessels. Angiogenesis depends on a delicate interplay between the endothelium and pericytes (2,3). Initially, tip cells migrate from the existing vessel and are followed by stalk cells, which divide and form a lumen, thus creating a capillary (4). The tip cell also

\*RCG, YWvdB, HHV, and VYB contributed equally to this work.

**Address correspondence to** Vladimir Y Bogdanov, Division of Hematology/Oncology, University of Cincinnati College of Medicine, 3125 Eden Avenue, Cincinnati, OH 45267. Phone: 513-558-6276; Fax: 513-558-6703; E-mail: [vladimir.bogdanov@uc.edu](mailto:vladimir.bogdanov@uc.edu); or Henri H Versteeg, Eindhoven Laboratory for Experimental Vascular Medicine, Leiden University Medical Center, Albinusdreef 2, 2333 ZA, Leiden, the Netherlands. Phone: +31-71-5263872; Fax: +31-71-5266755; E-mail: [h.h.versteeg@lumc.nl](mailto:h.h.versteeg@lumc.nl).  
Submitted October 27, 2011; Accepted for publication March 29, 2012; Epub (www.molmed.org) ahead of print April 2, 2012.

mediates recruitment of pericytes, which then align the capillary (5). This process is carefully regulated by key angiogenic molecules such as vascular endothelial growth factor (VEGF), platelet-derived growth factor, various metalloproteinases and interleukin-8 (6–8). However, angiogenesis also critically depends on integrin function. Integrins are heterodimeric receptors that are formed by the combination of 18 possible  $\alpha$ -subunits and 8  $\beta$ -subunits to form 20 separate extracellular matrix-binding receptors (9). These receptors, specifically  $\beta$ 1- and  $\beta$ 3-type integrins, play a critical role in endothelial cell and pericyte migration, but are also indispensable in the formation of capillaries (10,11). Although beneficial in certain physiologic settings, for example, embryonic development and wound healing, neovascularization is the *sine qua non* of primary tumor growth and metastasis, and in atherosclerosis, vasa vasorum is thought to be the major contributor to plaque instability (12).

Within the past decade, a soluble, naturally occurring TF splice variant (alternatively spliced tissue factor [asTF]) lacking a transmembrane domain was discovered (13). Absence of exon 5 in the mRNA of asTF results in an open reading frame shift, giving rise to a unique C-terminus. asTF can be secreted, exhibits minimal coagulant potential compared with the membrane-bound full-length TF (flTF) and is detectable, alongside flTF, in spontaneously formed arterial thrombi. Discernible procoagulant activity of native asTF was demonstrated to be low and phospholipid dependent (14); biosynthesis of asTF in monocytes and endothelial cells is controlled by several splicing regulator (SR) proteins, most notably ASF/SF2 and SRp55, and a group of kinases comprising Cdc2-like kinase, deoxyribonucleic acid (DNA) topoisomerase I and phosphatidylinositol 3-kinase (15–17). After the discovery of human asTF (hasTF), its murine homolog (masTF) was identified and characterized (18). Like hasTF, masTF lacks a transmembrane domain because of the exclusion of exon 5 from the primary tran-

script during pre-mRNA splicing and has a distinct 93-amino acid C-terminus, rendering it soluble. Whereas masTF was detected in abundance in organized arterial thrombi, as well as FeCl<sub>3</sub>-induced acute thrombi in mice systemically challenged with lipopolysaccharide (18,19), the functional contribution of masTF to any of the disease states that have been modeled *in vivo* (for example, tumorigenesis and atherothrombosis) has yet to be established (20).

We recently reported that hasTF induces angiogenesis and promotes monocyte-endothelial interactions via integrin ligation, without engaging protease activity (21,22). Thus, hasTF may be of interest in the field of anticancer therapies targeting neovascularization. Intriguingly, it was recently reported that overexpression of masTF in murine cardiomyocytes elicited increased production of promigratory and proangiogenic factors by these cells, although the molecular mechanisms underlying these effects of masTF were not fully ascertained (23). Because murine models comprise the preferred *in vivo* platform for cancer and cardiovascular research, it is imperative to determine whether masTF is a functional homolog of hasTF, especially with regard to nonproteolytic, integrin-mediated events promoting vessel growth.

Here we report for the first time that masTF possesses integrin-mediated biologic properties highly analogous to properties of hasTF, indicating that secreted variants of mammalian TF may generally act as agonists promoting neovascularization and monocyte recruitment via integrin ligation.

## MATERIALS AND METHODS

### Reagents and Antibodies

Murine TF isoform-specific polyclonal antibodies were described previously (12). An *in vitro* angiogenesis kit (Matrigel) was obtained from Millipore (Billerica, MA, USA). Anti-mouse  $\beta$ 1 (9EG7) and  $\beta$ 3 (2C9.G2) antibodies were from BD Pharmingen (Franklin Lakes, NJ, USA). Recombinant mouse VEGF was

purchased from Invitrogen (Carlsbad, CA, USA). Transwell permeable supports with 8  $\mu$ m pore size were from Costar (Corning, NY, USA). Isolectin B4 was from Vector Laboratories (Burlingame, CA, USA). Calcein-AM was from BD Biosciences (San Jose, CA, USA). Anti-murine p65/RelA polyclonal antibody was from Santa Cruz Biotechnology (Santa Cruz, CA, USA). SU5416 was from EMD Biosciences (San Diego, CA, USA). Rabbit anti-mouse Ccl-2 antibody was from Acris Antibodies (Herford, Germany). Recombinant ectodomain of murine flTF was produced and characterized as described (24).

### Immunohistochemistry

The *K-ras* induced the pancreatic ductal adenocarcinoma (PDAC) murine model, and atherosclerosis-prone *Ldlr*<sup>-/-</sup> mice were described previously (25,26). Serial sections of formalin-fixed, paraffin-embedded specimens were deparaffinized and rehydrated; endogenous peroxidase was blocked; and expression of masTF and mflTF was assessed using standard immunohistochemical techniques (22). Sections of murine atherosclerotic lesions were also assessed for masTF and mflTF colocalization with monocytes/macrophages by staining with anti-CD68 antibody (Santa Cruz Biotechnology).

### Generation of Recombinant asTF Proteins

N-terminally His-tagged recombinant hasTF was generated, purified and characterized as previously described (22). N-terminally His-tagged recombinant masTF mature protein was generated in *Escherichia coli*, purified, and assessed by Coomassie staining; the identity of masTF was confirmed by Western blotting (not shown).

### Cell Culture

Murine endothelial cells (ECs) (bEnd.3 from the American Type Culture Collection [ATCC], Manassas, VA, USA) and murine embryonic endothelial cells [MEECs], provided by MJ Goumans, Lei-

den University Medical Center [LUMC], Leiden, the Netherlands), primary human retinal endothelial cells (HRECs, Cell Systems) and murine monocytes/macrophages (J774A.1, ATCC) were grown in filter-cap tissue culture flasks containing Dulbecco's modified Eagle's medium (DMEM) supplemented with 10% fetal bovine serum (FBS) and penicillin/streptomycin (all from Hyclone/Thermo Scientific, Rockford, IL, USA). Incubators were maintained at 37°C and 5% CO<sub>2</sub>.

### EC Adhesion Assay

The 96-well plates were coated with 50 µL of 50 nmol/L masTF and 50 µL 10% bovine serum albumin (BSA) overnight. The  $2 \times 10^4$  bEnd.3 cells were added in 100 µL serum-free DMEM to each well for both conditions, and the plates then were placed in a 5% CO<sub>2</sub> incubator at 37°C for 4 h. The wells were washed with phosphate-buffered saline (PBS), and the adherent cells were fixed in methanol and stained with 0.1% crystal violet. In some experiments, 96-well plates were coated with 50 µL masTF at a concentration of 50 µg/mL, 10% BSA (negative control) or 1% gelatin (positive control) for 1 h at 37°C; subsequently, blocking was performed under the same conditions with 10% BSA. Then,  $2 \times 10^4$  bEnd.3 cells were seeded per well after 20-min incubation with integrin-blocking antibodies depending on the conditions at a concentration of 50 µg/mL. After 5 h, images were captured using a camera-equipped microscope, and flattened cells per view field were counted.

### EC Migration Assay

The lower sides of 8-µm pore transwell inserts were coated with 50 µL masTF at a concentration of 50 µg/mL for 1 h at 37°C, 10% BSA (negative control) or 1% gelatin (positive control). bEnd.3 cells or MEECs were trypsinized and incubated with integrin-blocking antibodies for 20 min at a concentration of 50 µg/mL when appropriate. The  $2 \times 10^4$  cells were seeded per well in DMEM containing 10% FBS and left to migrate overnight.

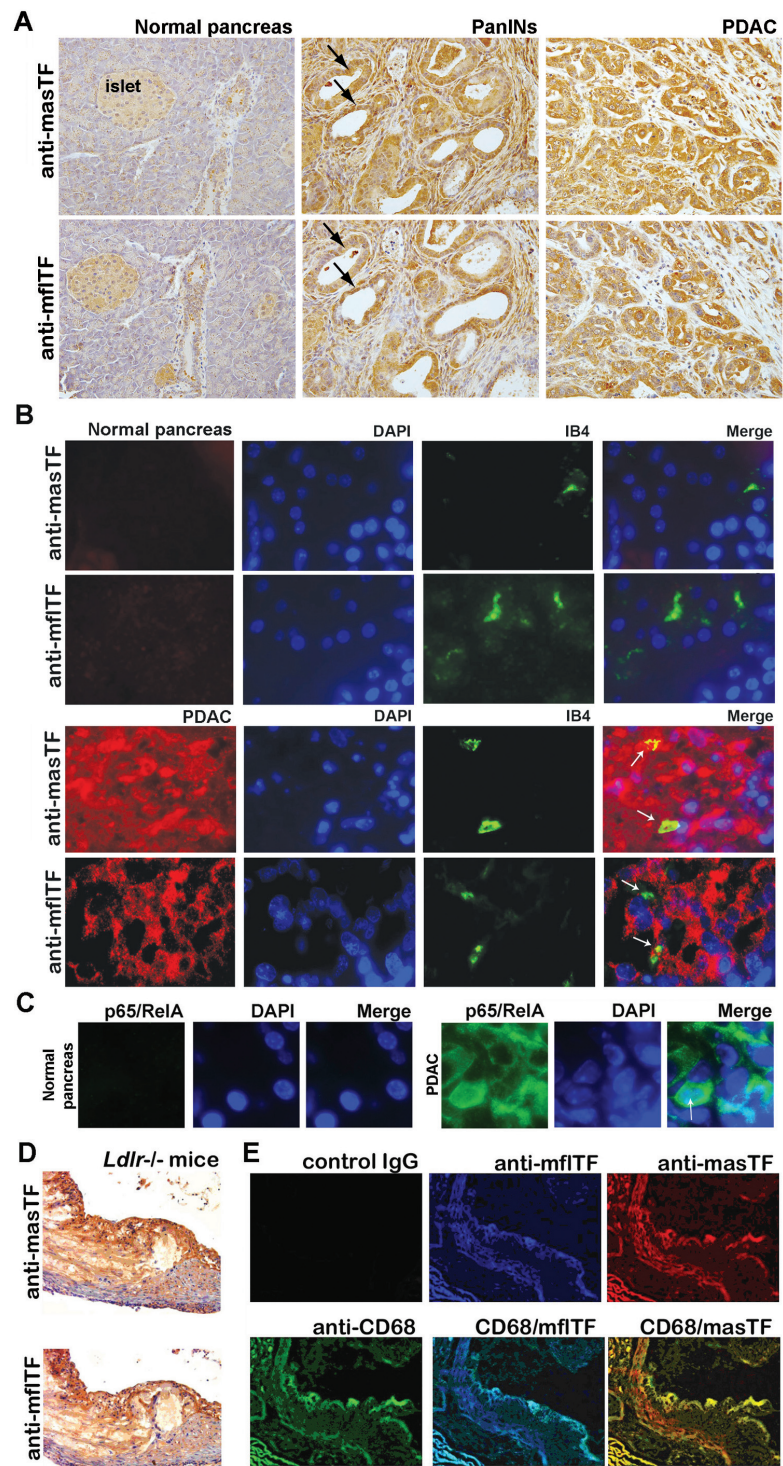


**Figure 1.** masTF is expressed in pancreatic cancer lesions and aortic plaques. (A, B) Presence and extensive colocalization of masTF and mfITF in serial sections of *K-ras*-induced murine PDAC lesions; white arrows denote microvessels in contact with masTF/mfITF-expressing cells and/or masTF-enriched stroma. (C) p65/RelA is expressed in PDAC tissue but not normal pancreas. (D) Presence of masTF and mfITF proteins in aortic plaques of *Ldlr*<sup>-/-</sup> mice. (E) masTF colocalizes with mfITF and CD68-positive cells within the plaques.

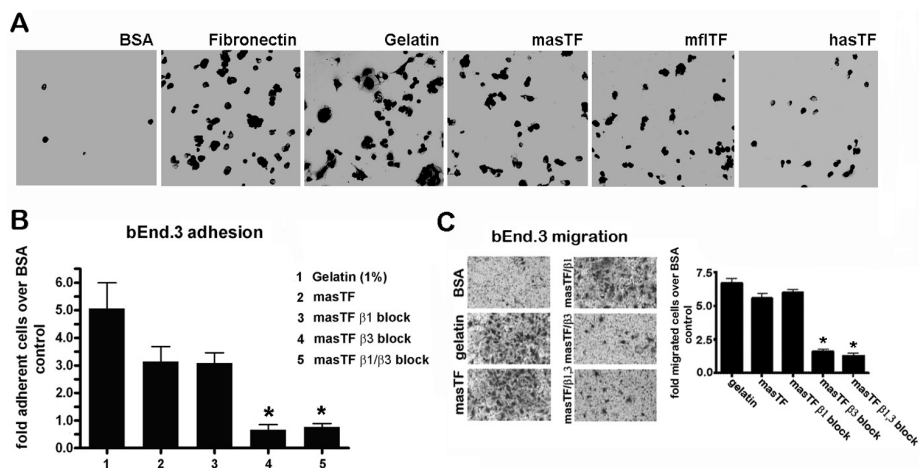


**Figure 2.** *masTF* binds  $\beta 3$  integrins on murine EC and elicits  $\beta 3$  integrin-dependent cell migration. (A) bEnd.3 cells avidly adhere to *masTF*, *mflTF* and *hasTF* ( $n \geq 6$ ). (B) bEnd.3 cells were pre-incubated with integrin-blocking antibodies and seeded onto BSA- or *masTF*-coated wells ( $n \geq 3$ ). Flattened cells were counted. (C) Transwell inserts were coated with BSA (negative control), 1% gelatin (positive control) and 50  $\mu\text{g}/\text{mL}$  *masTF*. Cells were fixed with 4% formaldehyde and stained with 0.1% crystal violet; quantifications are shown in the graph; representative images are on the left ( $n \geq 3$ ). \* $p < 0.01$ .

Filters were fixed in 4% phosphate-buffered formaldehyde, stained with crystal violet and washed in PBS; hereafter, cells on the top side of the filter were removed with a cotton swab. Microscope pictures were taken from the middle of the inserts, and cells were counted per magnification field. All experiments were performed in triplicate.

### Scratch Assay

bEnd.3 cells and HRECs were grown to confluence in six-well plates and maintained overnight in DMEM containing 2% FBS. Subsequently, eight radial scratches per well were introduced using a 20- $\mu\text{L}$  pipette tip. Cells were treated with *masTF*, *hasTF*, VEGF or PBS and glycerol (vehicle control) in 1 mL DMEM containing 10% FBS and incubated at 37°C, 5%  $\text{CO}_2$ . After 38 h, the cells were rinsed with PBS, fixed in methanol and stained with 0.1% crystal violet. The plates were placed on the platform of an inverted microscope, and pictures of a single radial wound (eight pictures per well) were captured at low magnification using a digital camera (SD1200IS, Canon). Analyses were carried out using

ImageJ software (U.S. National Institutes of Health, Bethesda, MD, USA; <http://imagej.nih.gov/ij/>). Pictures were converted to binary, the area of the cells was measured, and each wound area was then measured relative to the area of the cells. The area of the cells was used to normalize the area of the wound. Final pixilation of each scratch was converted to  $\text{mm}^2$ .

### Aortic Sprouting Assay

Male C57Bl/6 mice were obtained from Harlan Sprague-Dawley (Horst, the Netherlands) and were maintained at the animal care facility of the Leiden University Medical Center according to the institutional guidelines. Animal procedures were carried out in compliance with Institutional Standards for Humane Care and Use of Laboratory Animals. The Animal Care and Use Committee of the Leiden University Center approved all experiments. Mice ranging in age from 9 to 11 wks were sacrificed by cervical dislocation. Aortas were dissected, cleaned and flushed with serum-free RPMI-1640. Subsequently, aortas were cut into ~1-mm segments, embedded into 70  $\mu\text{L}$

Matrigel, and left in a 37°C incubator to polymerize. Matrigel was supplemented with *masTF*, *hasTF*, 5  $\mu\text{mol}/\text{L}$  SU5416 (VEGFR2 inhibitor), anti-Ccl2 antibody (final concentration 10.0  $\mu\text{g}/\text{mL}$ ) or buffer control depending on the experimental conditions. A 9:1 medium mixture of M199:EGM and 100  $\mu\text{g}/\text{mL}$  streptomycin and 100 units/mL penicillin was used to cover the embedded aortic segments. Integrin blockade was performed by addition of antibodies to the Matrigel at a concentration of 50  $\mu\text{g}/\text{mL}$ , when appropriate.

### Microarray Analysis

bEnd.3 cells were grown to confluence in six-well plates and treated with 50 nmol/L *masTF* (excluding controls) for 6 h; total RNA was extracted using a Qiagen RNeasy Mini Kit (Valencia, CA, USA), reverse-transcribed, amplified, fragmented and labeled for microarray analysis using the Nugen WT-Ovation FFPE V2 kit, Exon Module and Encore biotin module, respectively (Nugen), according to the manufacturer's instructions. An Affymetrix Gene 1.0 ST microarray platform was used to assess the gene expression profile (Microarray Core Facility, Cincinnati Children's Hospital and Medical Center). RNA transcripts were identified on the basis of filtering for probesets with Robust Multichip Average-normalized raw expression of  $>6.0$ , which differed between those treated with either *masTF* or *hasTF* and untreated ECs by at least 1.2-fold for up-regulated genes and at least 0.9-fold for down-regulated genes with  $p < 0.05$  by using a Welch  $t$  test. Using this approach, 338 probesets were identified that were differentially up-regulated, of which 133 were up-regulated and 205 were down-regulated. Of these 338 probesets, 264 genes were protein-coding genes (listed in Supplementary Table S1).

### Orbital Shear Assay

bEnd.3 cells and HRECs were grown to confluence in 96-well plates and treated with *masTF* or *hasTF* for 4 h. Subsequently, J774A.1 cells prelabeled

with Calcein-AM at 1  $\mu\text{mol/L}$  final concentration, washed free of unlabeled dye, were added at  $1 \times 10^5$  cells/well. The plates were placed on a horizontal orbital shaker and left rotating at 90 rpm in a 5%  $\text{CO}_2$  incubator at 37°C for 20 min. Nonadherent J774A.1 cells were washed away with PBS, adherent cells were lysed in PBS containing 0.5% Triton-X and fluorescence was measured at Ex-485 and Em-515.

All supplementary materials are available online at [www.molmed.org](http://www.molmed.org).

## RESULTS

### Expression of masTF and mflTF in Pancreatic Cancer Lesions and Colocalization with CD68-Positive Cells in Atherosclerotic Plaques

Expression of hasTF was detected in many PDAC cell lines, and hasTF was previously shown to promote tumor growth (27,28). We examined the expression patterns of masTF and mflTF in pancreatic tissue of genetically modified mice that spontaneously develop preneoplastic lesions (PanINs) and PDAC; as shown in Figure 1A, the intensity of staining for masTF as well as mflTF increased as lesions progressed from early PanINs to high-grade PDAC phenotype, indicating that masTF is likely to contribute to pancreatic tumor growth in the murine setting. Compared to mflTF, staining for masTF in PanINs and PDAC tissue appeared to be somewhat more diffuse; to ascertain whether masTF is present in the extracellular stromal compartment, immunofluorescence studies were performed and, as shown in Figure 1B, masTF was found in abundance in tumor cells as well as extracellular stroma, whereas mflTF was exclusively cell associated. *K-ras*-triggered upregulation of nuclear factor (NF)- $\kappa\text{B}$  is a well-established pathological feature of PDAC (29), and transcription of human as well as murine TF-encoding genes (*F3* and *Cf3*, respectively) is markedly responsive to NF- $\kappa\text{B}$ . Examination of murine pancreatic tissue for the levels of p65/RelA re-

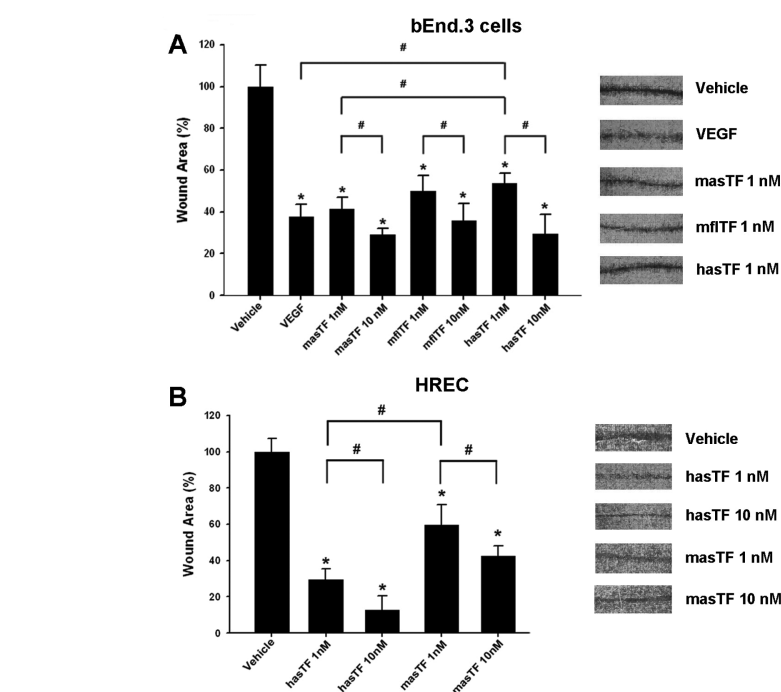


**Figure 3.** Effects of masTF and hasTF in the scratch assay. bEnd.3 cells (A) and HRECs (B) were grown to confluence in six-well plates and serum-starved overnight in DMEM containing 2% FBS. Eight radial scratches per well were introduced (see Materials and Methods). After 38 h, cells were washed with PBS, fixed in methanol and stained with 0.1% crystal violet. Representative images of the wounds are on the right ( $n \geq 4$ ). \* $p < 0.01$  versus vehicle; # $p < 0.05$ .

vealed that normal pancreas was negative, whereas PDAC tissue had high levels of p65/RelA, with some tumor cells exhibiting pronounced nuclear redistribution of p65/RelA (Figure 1C). Aside from neoplastic diseases, neovascularization plays a critical role in plaque remodeling (12). While we previously demonstrated that masTF is present in experimental occlusive thrombi in the wire injury model (17) and hasTF was detected in aortic plaques (22,30), it is not known whether masTF is present in aortic plaques. Appreciable levels of masTF were detectable in *Ldlr*<sup>-/-</sup> plaques (Figure 1D), where extensive colocalization of masTF with mflTF and CD68-positive cells was observed (Figure 1E).

### masTF and hasTF Bind Integrins on Murine ECs and Elicit Migration in a Transwell Assay

Because hasTF was previously shown to bind integrins, masTF may similarly

influence cell behavior through integrin ligation. To study this, tissue culture plates were coated with masTF, mflTF or hasTF and blocked with BSA, after which bEnd.3 cells were seeded. bEnd.3 cells avidly bound to masTF-, mflTF- and hasTF-coated plates, but bound poorly to BSA-coated plates (Figure 2A). To identify the possible involvement of integrins, bEnd.3 cells were pre-incubated with specific blocking antibodies. Inclusion of a  $\beta 3$  integrin-blocking antibody dramatically inhibited EC binding to masTF (Figure 2B). We previously showed that EC binding to hasTF is inhibited by  $\beta 1$  blockade. Nevertheless, binding of bEnd.3 cells to masTF was not disrupted by  $\beta 1$  blockade, and the combination of  $\beta 1$  and  $\beta 3$  blockades showed a similar reduction of cell adhesion when compared with a selective  $\beta 3$  blockade (see Figure 2B). Thus,  $\beta 3$  integrins (but not  $\beta 1$  integrins) appear to predominate in masTF-murine EC interactions. As we

previously showed that hasTF is a potent inducer of EC migration in a transwell migration assay, we sought to ascertain whether masTF protein exhibits similar properties. Indeed, a fivefold upregulation of bEnd.3 cell migration was observed in transwells that were coated with masTF. To determine the identity of the involved integrins, we treated ECs with integrin-blocking antibodies before the assay. As was observed before for hasTF, masTF-induced EC migration was shown to solely depend on  $\beta 3$  integrins (Figure 2C); analogous results were obtained when MEECs were used in this assay (Supplementary Figure S1).

### masTF and hasTF Are Potent Agonists in a Scratch Assay

Scratch assays are often used to assess cellular motility, invasion and intercellular interactions (31). To determine if, aside from the gradient-type/transwell system, masTF and/or hasTF are able to potentiate scratch closure, we used a scratch assay by using bEnd.3 cells and HRECs to assess the relative degree of potency. Per scratch, the enhancement of bEnd.3 closure by masTF (1 nmol/L) was not distinguishable from that elicited by VEGF (2 nmol/L, approximately twofold over vehicle control;  $p < 0.01$ , Figure 3A). The effects of mflTF (1 nmol/L) were similar to those of masTF, yet hasTF was less potent at 1 nmol/L; at 10 nmol/L, all three forms of TF exhibited similar potency (see Figure 3A). When HRECs were used in the scratch assay, hasTF was markedly more potent than masTF in the 1–10 nmol/L range (Figure 3B).

### masTF Induces Vessel Growth *Ex Vivo*

Because hasTF mediates angiogenesis and the biologic effects of masTF observed *in vitro* are in line with the *in vitro* effects of hasTF, we next assessed whether masTF promotes angiogenesis *ex vivo*. Using aortic sprouting assays, we confirmed that masTF induces the formation of new vessels with the levels of potency indistinguishable from that of hasTF in the 1–100 nmol/L range (Fig-

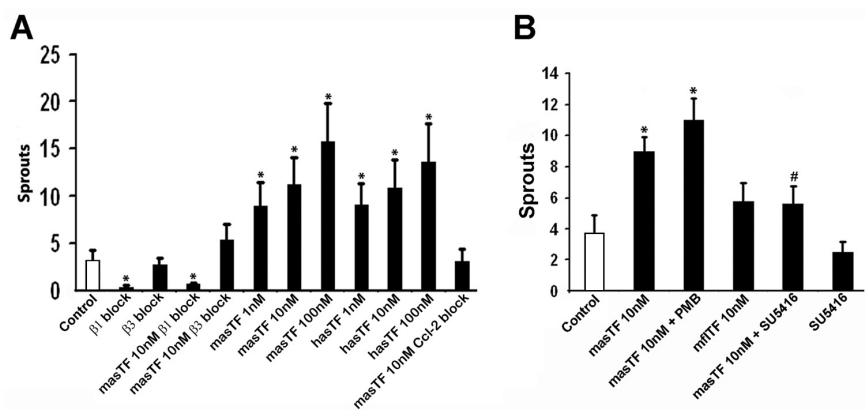


**Figure 4.** masTF induces aortic sprouting. Murine thoracic aortas were isolated and cleaned of the surrounding tissue in serum-free RPMI-1640 containing 100 units/mL penicillin and 100  $\mu$ g/mL streptomycin. Dissected aortas were flushed with PBS; sectioned into equal segments; and embedded in matrigel supplemented with solvent control, masTF, hasTF or mflTF. Integrin/Ccl2-blocking antibodies (A) or SU5416 (VEGF inhibitor, B) were included in the matrigel when appropriate. PMB, polymyxin B. Sprouts were counted on d 4 ( $n \geq 4$ ). \* $p < 0.01$  versus control.

ure 4A). Next, we determined whether masTF-induced *ex vivo* angiogenesis is integrin dependent, and we indeed observed sprouting comparable to basal levels in the presence of  $\beta 3$  blocking antibodies; however, a  $\beta 1$  blockade also resulted in downregulation of *ex vivo* angiogenesis, in the absence as well as the presence of exogenously added masTF (Figure 4A). Because Matrigel consists primarily of  $\beta 1$  integrin–ligating extracellular matrix proteins, it is plausible that the synergy between  $\beta 1$ -ligating matrigel and  $\beta 3$ -ligating masTF is required for the masTF-dependent formation of sprouts and, as such, masTF possesses angiogenic properties analogous to those of hasTF. Strikingly, antibody blockade of Ccl2—a chemokine recently shown to be critical for flTF-mediated angiogenesis (32)—completely eliminated the effect of masTF, indicating that Ccl2 is indispensable for masTF-mediated proangiogenic effects (see Figure 4A). However, VEGF blockade, while diminishing the basal angiogenesis, did not eliminate the proangiogenic effects of masTF in this assay (Figure 4B). We note that we detected low levels of endogenous masTF protein in our Matrigel cultures by Western blotting (data not shown). When

mflTF ectodomain was added to the cultures, there appeared to be a weak increase in sprouting that did not reach statistical significance (see Figure 4B).

### masTF and hasTF Elicit Analogous Changes in the Global Expression Profile of Murine ECs

Although the signaling events elicited by hasTF in human ECs were investigated previously (22), nothing is known about the changes in gene expression in murine ECs elicited by masTF. bEnd.3 cells stimulated with masTF and hasTF revealed significant nuclear redistribution of p65/Rel A (Figure 5A). Microarray analysis revealed that hasTF and masTF exert similar effects on global gene expression in murine ECs (Figure 5B). A significant number of genes were upregulated as well as downregulated by both masTF and hasTF; the list of these genes is presented in Supplementary Table S1. The major genes that were significantly upregulated were chemokine family genes, such as *Cxcl2*, *Csf-1* and *Ccl2*. Integrin-linked kinase (ILK) is a binding partner for  $\beta 1$  and  $\beta 3$  integrins and helps in anchoring  $\beta 1$  and  $\beta 3$  integrins to the actin cytoskeleton. ILK-mediated signaling has been shown

to significantly upregulate *SDF1* (*Cxcl12*) expression in human ECs (33). Because we established that hasTF, and now masTF, ligate integrins, these TF variants could well trigger ILK-dependent signaling in murine ECs. Analogously to human microvascular ECs, for which exposure to hasTF resulted in the upregulation of NF- $\kappa$ B pathway-related chemokines (22), hasTF and masTF elicited activation of NF- $\kappa$ B-dependent pathways in murine ECs (see Figure 5B).

### masTF and hasTF Promote Monocyte Adhesion to Murine ECs

Whereas the expression of cell adhesion molecules on murine ECs was not upregulated as dramatically in response to masTF and/or hasTF as was shown for human ECs (22), *Vcam-1* (the gene encoding an adhesion molecule critical to EC-monocyte interactions) was upregulated by ~6.5-fold in response to both masTF and hasTF (Supplementary Table S1, Figure 6A), which is significant, since even a modest increase in the levels of VCAM-1 reflects a state of activated endothelium (34). Having established that masTF, like hasTF, is present in aortic plaques and induces the expression of chemokines in murine EC (Figures 1, 5), we sought to determine whether masTF promotes adhesion of murine monocytes to murine and/or human ECs. As shown in Figures 6B and C, masTF as well as hasTF elicited a significant increase in the adhesion of murine monocytes to bEnd.3 cells and HREC under orbital shear conditions.

### DISCUSSION

While the importance of the TF-integrin axis has been known for some time, it has been shown that the fITF-integrin cross-talk primarily involves  $\beta$ 1, not  $\beta$ 3 integrins (1); thus,  $\beta$ 3-mediated events may very well be uniquely regulated by asTF in human as well as murine solid tissues. Strikingly, murine ECs do not appear to engage  $\beta$ 1 integrins while adhering to masTF (Figure 2), yet both  $\beta$ 1 and  $\beta$ 3 integrins are required for masTF-elicited angiogenesis, analogously to the

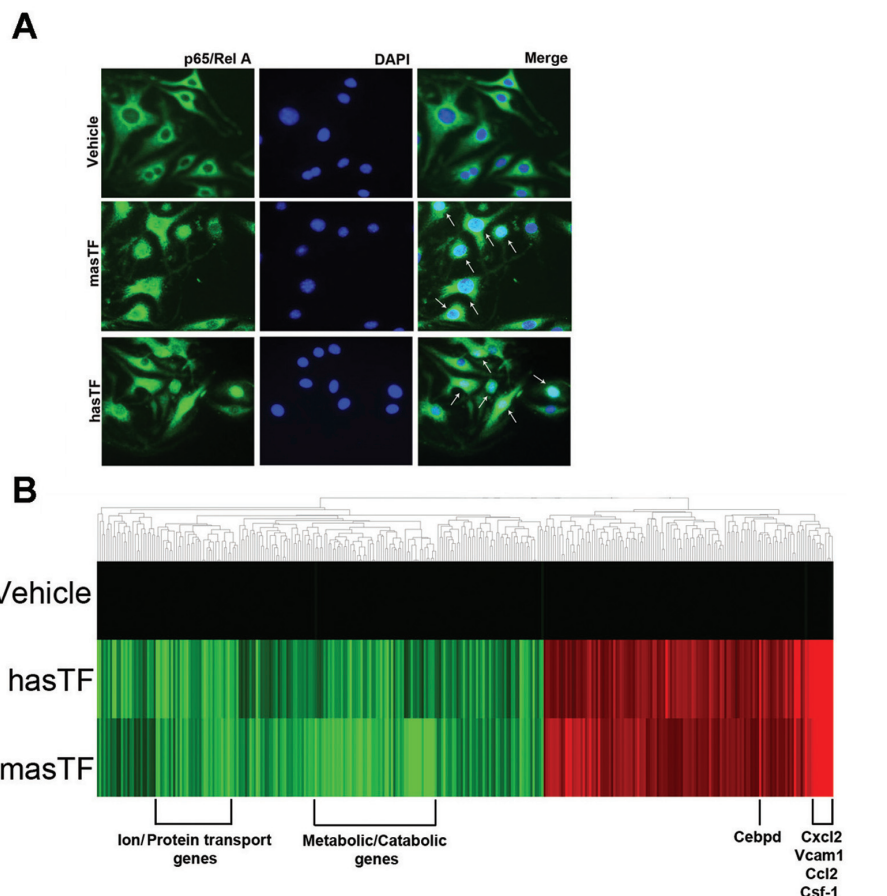


**Figure 5.** masTF and hasTF elicit analogous changes in the gene expression profile of murine ECs. (A) Cellular distribution of p65/RelA in bEnd.3 cells stimulated with masTF and hasTF ( $n \geq 3$ ). White arrows indicate nuclear localization. (B) Heat map, gene cluster analysis of bEnd.3 cells exposed to 50 nmol/L of masTF and 50 nmol/L of hasTF for 4 h; 50% glycerol/PBS served as vehicle control. The heat map comprises the genes for which expression was either significantly upregulated by at least 1.2-fold or downregulated by at least 0.9-fold. Results shown are representative of three independent experiments; red denotes upregulation and green denotes downregulation.

hasTF (Figure 4) (21). It should be noted that  $\beta$ 3-deficient mice exhibit a pathological enhancement of angiogenesis rather than inhibition of vessel growth (35); however, aberrations triggered by global  $\beta$ 3 deficiency may not be reflective of the effects elicited by soluble  $\beta$ 3 ligands (for example, masTF/hasTF) in select tissue subcompartments (for example, the vasculature). Whereas it cannot be excluded that the relative abundance of  $\beta$ 1 versus  $\beta$ 3 integrins may influence experimental outcomes in studies involving distinct EC lines/subtypes (22), the differences in global gene expression changes elicited

by hasTF in human ECs and masTF in murine ECs are also likely to play a role. The divergence of the gene expression cascades notwithstanding, the end results of masTF-murine EC interactions, that is, angiogenesis and monocyte recruitment, are remarkably analogous to those of hasTF-human EC interactions. The structure of the unique C-terminus of asTF is another aspect of asTF biology that may explain the differential “integrin profiles” of masTF and hasTF. masTF has a longer C-terminal domain than hasTF and may confer a distinct, masTF-unique conformation, resulting in the activation of a

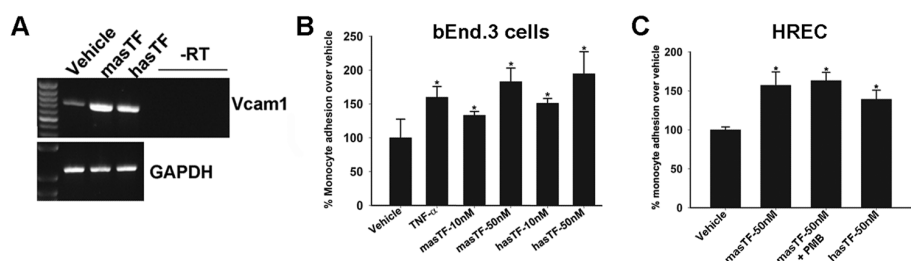


**Figure 6.** masTF and hasTF promote monocyte adhesion to murine ECs. (A) Reverse transcriptase (RT)-polymerase chain reaction expression of *Vcam-1* in masTF/hasTF-stimulated bEnd.3 cells. (B, C) Representative experiment ( $n = 3$ ), orbital shear assay performed using bEnd.3 cells (B) or HRECs (C) and prelabeled J7741.A cells. PMB, polymyxin B. \* $p < 0.01$ .

different subset of integrins. We note that *in silico* searches for potential integrin-binding sites within unique C-termini of hasTF and masTF did not yield any candidate motifs (RC Godby, R Srinivasan, VY Bogdanov, unpublished data); thus, further studies on the functional role(s) of the hasTF and masTF C-termini and its physiological implications are warranted.

Our findings are in agreement with those of other groups who recently reported upregulation of such proangiogenic molecules as VEGF, basis fibroblast growth factor (bFGF) and Cyr61 as a result of masTF overexpression in murine cardiomyocytes (23,36); the VEGF-independent nature of masTF-elicited effects in the sprouting assay and the gene array analysis suggest that murine ECs may react to masTF in ways not fully identical to those observed in cardiac tissue (Figures 4, 5). *Cxcl2* (a gene analogous to *Il-8*) encodes a major inflammatory chemokine involved in the recruitment of inflammatory cells (37,38), whereas *Csf-1* production by stromal cells has been linked to the increased recruitment of tumor-associated macrophages and propagation of metastases (39). Genes encoding regulatory transcription factors were also upregulated in masTF- and hasTF-treated cells, for example, *Cebpd* and *Cebpb*. We note that *Cebpd* is involved in tumor suppression, and its increased expression might be due to a feedback response to the upregulation of inflammatory/tumor-activating genes. Interestingly, the expression of

*Gja5* (the gene encoding a gap junction protein for which loss is associated with decreased endothelial relaxation and eNOS levels in the mouse aorta [40]) was downregulated by masTF and hasTF, raising the possibility that the effects of these soluble TF variants may exacerbate systemic vasculopathies related to aberrant eNOS activity.

While we are currently dissecting what signaling cascades are engaged by masTF in murine ECs, the results of our study clearly demonstrate that there are many similarities between masTF and hasTF when it comes to their targets. It is worth noting that  $\beta3$  integrins play a comparably crucial role in cardiovascular disease and cancer—the conditions hallmarked by chronic inflammatory events, a common feature in the pathobiology of atherosclerosis and solid malignancies (41,42). As the levels of masTF rise during pancreatic cancer progression (Figure 1), it is worth noting that  $\alpha v\beta3$ —the integrin known to interact with hasTF—plays a particularly major role in pancreatic cancer pathobiology. The  $\alpha v\beta3$  dimer, a major RGD receptor, is perceived to exert its tumor-promoting effects through adhesion-mediated modulation of tumor cell invasiveness and proliferative/migratory capacity, as well as promoting metastatic neovascularization: compared with normal microvessels, metastatic microvessels express higher levels of this integrin (43). However,  $\alpha v\beta3$  is also expressed in PDAC cells and was reported to play a signifi-

cant adhesion-independent role in pancreatic cancer (44). masTF appears to act as a cell agonist by ligating  $\beta3$  integrins on ECs, which activates the NF- $\kappa$ B pathway (Figure 5A). The  $\beta3$ -asTF nexus may thus promote tumorigenesis directly via autocrine stimulation of cancer cells, as well as indirectly via neovascularization. The tenet that the flTF/asTF synergy promotes primary tumor growth, and possibly spread, is supported by the effects of monoclonal antibody 10H10, an flTF-specific antibody that disrupts constitutive binding of flTF to integrins and also inhibits tumor growth in xenograft models (45). Moreover, the Ccl2-dependent nature of masTF-elicited angiogenesis further supports the notion that asTF and flTF are likely to act in concert to trigger the formation of new vessels, using proteolytic as well as non-proteolytic signaling (32). Inasmuch as exogenous flTF on microparticles and lipid vesicles stimulates cell proliferation largely in a  $\beta1$  integrin-dependent manner (46), it is reasonable to propose that asTF similarly promotes integrin-mediated tumorigenesis, yet with a far more pronounced engagement of  $\beta3$  integrins. Future experiments should reveal whether asTF acts as a proangiogenic as well as mitogenic agent *in vivo*.

## CONCLUSION

The major novel findings we report here are as follows: (a) masTF is biologically active; (b) the biologic effects of masTF are analogous to those of hasTF and can be experimentally assessed using murine as well as human cell cultures; and (c) masTF-mediated angiogenesis depends on  $\beta1$  and  $\beta3$  integrins as well as Ccl-2, yet is independent of VEGF. Specifically, we show for the first time that the murine form of asTF is a functional homolog of hasTF inasmuch as it acts as an agonist on EC surfaces in promoting cell adhesion, migration and neovascularization in an integrin-mediated fashion.

## ACKNOWLEDGMENTS

This study was partially supported by National Institutes of Health (NIH) grant



HL094891 to VY Bogdanov, NIH grant CA124586 to SF Konieczny and the Netherlands Organization for Scientific Research (NWO grant 17.106.329 to HH Versteeg).

## DISCLOSURE

The authors declare that they have no competing interests as defined by *Molecular Medicine*, or other interests that might be perceived to influence the results and discussion reported in this paper.

## REFERENCES

- Versteeg HH, Ruf W. (2006) Emerging insights in tissue factor-dependent signaling events. *Semin. Thromb. Hemost.* 32:24–32.
- Armulik A, Abramsson A, Betsholtz C. (2005) Endothelial/pericyte interactions. *Circ. Res.* 97:512–23.
- Carmeliet P, Jain RK. (2011) Molecular mechanisms and clinical applications of angiogenesis. *Nature.* 473:298–307.
- Holderfield MT, Hughes CC. (2008) Crosstalk between vascular endothelial growth factor, notch, and transforming growth factor-beta in vascular morphogenesis. *Circ. Res.* 102:637–52.
- Gaengel K, Genové G, Armulik A, Betsholtz C. (2009) Endothelial-mural cell signaling in vascular development and angiogenesis. *Arterioscler. Thromb. Vasc. Biol.* 29:630–8.
- Ferrara N, Gerber HP, Lecouter J. (2003) The biology of VEGF and its receptors. *Nat. Med.* 9:669–76.
- Rundhaug JE. (2005) Matrix metalloproteinases and angiogenesis. *J. Cell Mol. Med.* 9:267–85.
- Li A, Dubey S, Varney ML, Dave BJ, Singh RK. (2003) IL-8 directly enhanced endothelial cell survival, proliferation, and matrix metalloproteinases production and regulated angiogenesis. *J. Immunol.* 170:3369–76.
- Hynes RO. (2002) Integrins: bidirectional, allosteric signaling machines. *Cell.* 110:673–87.
- Brooks PC, Clark RA, Cheresh DA. (1994) Requirement of vascular integrin alpha v beta 3 for angiogenesis. *Science.* 264:569–71.
- Bloch W, et al. (1997) Beta 1 integrin is essential for teratoma growth and angiogenesis. *J. Cell Biol.* 139:265–78.
- Galis ZS, Lessner SM. (2009) Will the real plaque vasculature please stand up? Why we need to distinguish the vasa plaquorum from the vasa vasorum. *Trends Cardiovasc. Med.* 19:87–94.
- Bogdanov VY, et al. (2003) Alternatively spliced human tissue factor: a circulating, soluble, thrombogenic protein. *Nat. Med.* 9:458–62.
- Szotowski B, Antoniak S, Poller W, Schultheiss HP, Rauch U. (2005) Procoagulant soluble tissue factor is released from endothelial cells in response to inflammatory cytokines. *Circ. Res.* 96:1233–9.
- Tardos JG, et al. (2008) SR proteins ASF/SF2 and SRp55 participate in tissue factor biosynthesis in human monocytic cells. *J. Thromb. Haemost.* 6:877–84.
- Eisenreich A, et al. (2009) Cdc2-like kinases and DNA topoisomerase I regulate alternative splicing of tissue factor in human endothelial cells. *Circ. Res.* 104:589–99.
- Eisenreich A, et al. (2009) Role of the phosphatidylinositol 3-kinase/protein kinase B pathway in regulating alternative splicing of tissue factor mRNA in human endothelial cells. *Circ. J.* 73:1746–52.
- Bogdanov VY, et al. (2006) Identification and characterization of murine alternatively spliced tissue factor. *J. Thromb. Haemost.* 4:158–67.
- Brüggenmann LW, Drijfhout JW, Reitsma PH, Spek CA. (2006) Alternatively spliced tissue factor in mice: induction by *Streptococcus pneumoniae*. *J. Thromb. Haemost.* 4:918–20.
- Srinivasan R, Bogdanov VY. (2011) Alternatively spliced tissue factor: discovery, insights, clinical implications. *Front Biosci.* 17:3061–71.
- van den Berg YW, et al. (2009) Alternatively spliced tissue factor induces angiogenesis through integrin ligation. *Proc. Natl. Acad. Sci. U. S. A.* 106:19497–502.
- Srinivasan R, et al. (2011) Splice variants of tissue factor promote monocyte-endothelial interactions by triggering the expression of cell adhesion molecules via integrin-mediated signaling. *J. Thromb. Haemost.* 9:2087–96.
- Eisenreich A, Boltzen U, Malz R, Schultheiss HP, Rauch U. (2011) Overexpression of alternatively spliced tissue factor induces the pro-angiogenic properties of murine cardiomyocytic HL-1 cells. *Circ. J.* 75:1235–42.
- Disse OJ, et al. (2011) The endothelial protein C receptor supports tissue factor ternary coagulation initiation complex signaling through protease-activated receptors. *J. Biol. Chem.* 286:5756–67.
- Habbe N, et al. (2008) Spontaneous induction of murine pancreatic intraepithelial neoplasia (mPanIN) by acinar cell targeting of oncogenic Kras in adult mice. *Proc. Natl. Acad. Sci. U. S. A.* 105:18913–8.
- Swertfeger DK, Bu G, Hui DY. (2002) Low density lipoprotein receptor-related protein mediates apolipoprotein E inhibition of smooth muscle cell migration. *J. Biol. Chem.* 277:4141–6.
- Haas SL, et al. (2006) Expression of tissue factor in pancreatic adenocarcinoma is associated with activation of coagulation. *World J. Gastroenterol.* 12:4843–9.
- Hobbs JE, et al. (2007) Alternatively spliced human tissue factor promotes tumor growth and angiogenesis in a pancreatic cancer tumor model. *Thromb. Res.* 120 (Suppl. 2):S13–21.
- Pan X, et al. (2008) Nuclear factor-kappaB p65/relA silencing induces apoptosis and increases gemcitabine effectiveness in a subset of pancreatic cancer cells. *Clin. Cancer Res.* 14:8143–51.
- van den Berg YW, Versteeg HH. (2010) Alternatively spliced tissue factor: a crippled protein in coagulation or a key player in non-haemostatic processes? *Haemostaseologie.* 30:144–9.
- Rodriguez LG, Wu X, Guan JL. (2005) Wound healing assay. *Methods Mol. Biol.* 294:23–9.
- Arderiu G, Peña E, Aledo R, Juan-Babot O, Badimon L. (2011) Tissue factor regulates microvessel formation and stabilization by induction of chemokine (C-C motif) ligand 2 expression. *Arterioscler. Thromb. Vasc. Biol.* 31:2607–15.
- Lee SP, et al. (2006) Integrin-linked kinase, a hypoxia-responsive molecule, controls postnatal vasculogenesis by recruitment of endothelial progenitor cells to ischemic tissue. *Circulation.* 114:150–9.
- Nakashima Y, Raines EW, Plump AS, Breslow JL, Ross R. (1998) Upregulation of VCAM-1 and ICAM-1 at atherosclerosis-prone sites on the endothelium in the ApoE-deficient mouse. *Arterioscler. Thromb. Vasc. Biol.* 18:842–51.
- Reynolds LE, et al. (2002) Enhanced pathological angiogenesis in mice lacking beta3 integrin or beta3 and beta5 integrins. *Nat. Med.* 8:27–34.
- Boltzen U, et al. (2012) Alternatively spliced tissue factor and full-length tissue factor protect cardiomyocytes against TNF- $\alpha$ -induced apoptosis. *J. Mol. Cell Cardiol.* 52:1056–65.
- Tsujimoto H, et al. (2005) Flagellin enhances NK cell proliferation and activation directly and through dendritic cell-NK cell interactions. *J. Leukoc. Biol.* 78:888–97.
- Mancardi S, et al. (2003) Evidence of CXC, CC and C chemokine production by lymphatic endothelial cells. *Immunology.* 108:523–30.
- Abraham D, et al. (2010) Stromal cell-derived CSF-1 blockade prolongs xenograft survival of CSF-1-negative neuroblastoma. *Int. J. Cancer.* 126:1339–52.
- Alonso F, Boitton FX, Bény JL, Haefliger JA. (2010) Loss of connexin40 is associated with decreased endothelium-dependent relaxations and eNOS levels in the mouse aorta. *Am. J. Physiol. Heart Circ. Physiol.* 299:H1365–73.
- Burtea C, et al. (2008) Molecular imaging of alphav beta3 integrin expression in atherosclerotic plaques with a mimetic of RGD peptide grafted to Gd-DTPA. *Cardiovasc. Res.* 78:148–57.
- Couzin-Frankel C. (2010) Inflammation bares a dark side. *Science.* 330:1621.
- Rüegg C, Alghisi GC. (2010) Vascular integrins: therapeutic and imaging targets of tumor angiogenesis. *Recent Results Cancer Res.* 180:83–101.
- Desgrosellier JS, et al. (2009) An integrin alpha(v)beta(3)-cSrc oncogenic unit promotes anchorage-independence and tumor progression. *Nat. Med.* 15:1163–9.
- Versteeg HH, et al. (2008) Inhibition of tissue factor signaling suppresses tumor growth. *Blood.* 111:190–9.
- Collier ME, Ettelaie C. (2010) Induction of endothelial cell proliferation by recombinant and microparticle-tissue factor involves beta1-integrin and extracellular signal regulated kinase activation. *Arterioscler. Thromb. Vasc. Biol.* 30:1810–7.